Journal of Simulation and Analysis of Novel Technologies in Mechanical Engineering
16 (2) (2024) 0069~0082
DOI 10.71939/jsme.2024.1119530

Research article

Investigation the weld quality characterizations and temperature field in laser welding of dissimilar Nickle-base alloy Inconel 600 and duplex stainless steel

Ahmad Soleimani[1], Mohammad Akbari[1,2] *, Arash Karimipour[1,2], Amir Homayoon Meghdadi Isfahani[1,2] , Reza Nosouhi[1,3]

1-Department of Mechanical Engineering, Najafabad Branch, Islamic Azad University, Najafabad, Iran
2- Aerospace and Energy Conversion Research Center, Najafabad Branch, Islamic Azad University, Najafabad, Iran
3-Modern Manufacturing Technologies Research Center, Najafabad Branch, Islamic Azad University, Najafabad, Iran

* m.akbari.g80@gmail.com

(Manuscript Received --- 11 May 2024; Revised --- 28 June 2024; Accepted --- 03 Aug. 2024)

Abstract

Laser welding of dissimilar materials joint composed of Inconel 600 superalloy and stainless steel of duplex 2205 was performed via experimental design to analyze the weld quality characterization including the weld penetration depth and width and the microstructural variation at different regions of the weld bead. The process parameters impact on the temperature gradient near the boundary line of the fusion zone and base metals of both material according to the variation of focal distance, beam deviation direction to each material and welding speed were investigated. Additionally, variation in weld bead width, depth of weld penetration and appearance of weld bead surface were investigated according to the mentioned process parameters. The results imply that by moving the laser beam in direction of the duplex steel the width of the melt pool was more than that of super alloy 600. Due to the laser beam's high energy density and the melt pool depth remained relatively unchanged when welding at the focal point, as opposed to welding at higher focal distances. With the interaction effect of laser beam deflection of towards the Inconel 600 and increasing focal length due to a lower absorption coefficient and a significant reduction in energy density, the maximum reduction rate of molten pool depth was observed. The maximum weld bead width occurs at the place of laser beam radiation at the center line of the of two parts junction. The melt pool penetration depth has been reduced by approximately 50 percent by increasing the focal length about 2mm and specifically altering the laser beam's deviation in direction of the Inconel 600 super alloy. The maximum temperature for duplex steel is vividly higher than Inconel 600 about 20°C at a distance of 2mm from the melt pool center.

Keywords: Dissimilar materials, Laser welding, Inconel 600 superalloy, Duplex stainless steel, Molten pool, Temperature measurement, Weld geometry, Fusion zone microstructure.

1- Introduction

Different combinations of the Nickel based super alloys and stainless steels either austenitic martensitic or duplex in dissimilar welding have attracted considerable interest in field of gas turbines, aero engine parts and manufacturing of parts in chemical sectors is carried out due to the exceptional mechanical characteristics and resistance to corrosion exhibited by these components. [1-4]. Laser welding offers several important benefits, such as grain refinement and reduced residual stress, ultimately enhancing the overall quality of the weld [4-6]. Wu and colleagues explored the water cooling influence on the process of solidification during laser welding at pulsed for Inconel 600 Nickel-based alloy and austenitic stainless steel dissimilar joint with filler wire. Their objective was to enhance the mechanical properties of the laser-welded connections. The outcomes indicated that the use of water cooling resulted in an enhanced rate of cooling and sharp temperature gradient within the weld area. Moreover, the implementation of water cooling facilitated constitutional super-cooling, leading to a rise in the solidification rate corresponding to the temperature gradient [6]. Naffakh et al. evaluated the effect of using different filler materials for welding of dissimilar welding of AISI 304 and Inconel 657 (nickel and chromium base superalloy). Different nickel-based alloys with 310 austenitic stainless steels have formed dissimilar joint. The mechanical properties of the dissimilar joints and hot-cracking according to using different welding consumables fillers were analyzed. They utilized different Nickle base alloys including Inconel A, Inconel 617 and Inconel 82. The results illustrated that the highest strength and total elongation gained for Inconel A weldment while the weldment of Inconel 657 failed from parent metal. All of the weld metals failed under the ductile fracture mechanism except Inconel 617, which failed under the mixed fracture mode [7]. Zhou et al studied the effect of asymmetric laser beam energy distribution on dissimilar weld of (C-276) Nickel-based alloy and stainless steel 304. They proposed a relation between ratio of the irradiated energy on the C-276 alloy and the portion of C-276 alloy melted material, microstructural changes at different regions of the fusion zone, the corrosion resistance and the dissimilar weld mechanical properties. The weld microstructure mainly comprised the austenite phase in each weld, suppressing the formation of the δ-ferrite phase and promoting the intermetallic phase as EC-276 increased. The tensile strength of the weld joint increased by the strengthening elements of Mo and W. The dissimilar weld corrosion resistance was improved by increasing EC-276 due to existing the Mo element [8].

Dissimilar joint of Inconel 718 and AISI 416 martensitic stainless steel by been studied by Dev el al. They used a gas Tungsten Arc Welding at pulsed mode as means of the heat source and different filler materials including ERNiCrMo-4, ERNiCu-7 and duplex filler ER2553. It was reported that the weld failure was observed at AISI 416 under the tensile tests. The best affect toughness gained by using ERNiCu-7 filler metal [9]. Cheng et al. investigated the laser welded joints corrosion resistance and defects in dissimilar laser welding process of Hastelloy C-276 and 304 stainless steel with filler wire. The results of their study revealed that the inclusion of cooling rate

at low levels of the temperature improves the rate at which the weld cools down and solidifies. Additionally, by increasing the temperature difference near the fusion line of the weld and accelerating the solidification process, the amount of precipitated phase decreases by approximately 59.0%. Additionally, the increase in temperature gradient leads to a decrease in the unmixed zone, which reduces nearly 48.0%. At the same time, laser welding combined with low-temperature cooling demonstrates elevated levels of corrosion-resistant components and a greater concentration of grain boundaries featuring minor angles [10]. Kumar et al. investigated the effect of heat input on the microstructure and mechanical properties of different Nickle base alloys. The results show that the weld microstructures under different heat input process parameters display distinct characteristics, such as unmixed islands, dendritic grains featuring thin heat-affected regions, and reaction compounds abundant in Cr-carbides. Heat input variation created by using different welding speed, pulse energy levels and pulse duration in millisecond order. The joint tensile strength diminishes from the maximum level as the heat input rises [11]. Kumar et al evaluated the laser welding process parameters impact on geometry of the welded bead. The parameters were analyzed using Response Surface Methodology (RSM) to determine their parameters effects including welding power, welding speed, focal position, beam angle and beam offset on the depth of penetration (DP), weld bead width and the penetration area [12]. The statistical results indicated that the welding power and welding speed play a crucial role in determining the strength of dissimilar joints. The beam angle has little effect on bead width, Fusion Zone region and the beam offset does not have a significant impact on bead width [12]. In another study, the analysis focused on examining the mechanical properties and microstructural changes in joints of stainless steel 304 and Inconel 718, both in similar and dissimilar configurations, as observed. The investigation primarily compared two mechanical properties, namely tensile strength and hardness. The dissimilar Inconel-stainless steel joint has demonstrated a favorable combination of tensile strength and hardness. The ultimate tensile strength that is 14% higher than similar stainless steel joints and 13% lower than similar Inconel joint. Moreover, the hardness of the dissimilar joint is comparable to that of the stainless steel plate [13]. Bhanu et al investigated dissimilar laser welding of p91 steel and incoloy 800ht nickel alloy microstructure and mechanical properties. The highest level of penetration through the keyhole mode was attained through the utilization of the single-pass laser welding method. The weld fusion zone microstracture exhibited solidification cracks and the susceptibility of Incoloy 800HT to these cracks resulting from a difference in melting point and thermal conductivity of the base materials. The results of the tensile test for standard welding specimen revealed failure from the base metal, with a yield stress of 265 MPa. The post-weld heat treatment increased the yield stress up to 297 MPa [14]. Dak and Pandey conducted a research on the dissimilar laser beam welded joint between 304L austenitic stainless steel and martensitic P92 steel. They examined both the as-welded condition and the impact of post-weld heat treatment. A detailed study of the

microstructure at different weld regions including heat-affected zone and weld fusion zone interface revealed significant levels of inhomogeneity within the dissimilar joint.The mechanical properties according to inhomogeneity impact indicated a slight increase in tensile strength from 587.709 MPa to 594.515 MPa from as weld to PWHT condition. After the post heat treatment, it was observed that the residual stresses from both circumferential and axial stress welding were reduced, as indicated by the results. [15]. Thejasree et al. assessed the mechanical characterization of the laser welded thin sheets of Inconel 718 alloy via Laser welding. The weldments characterizations including tensile strength and hardness illustrated better properties. [16].

This research introduces a novel experimental method for dissimilar laser welding between duplex 2205 stainless steel and Nickle base superalloy Inconel 600. This paper focused on the dissimilar weld geometry, temperature field and microstructural changes related to dissimilar welding because of having different melting point, chemical composition, thermal and mechanical properties and thereby forming unmixed zone, elemental segregation and other microstructural changes. An evident correlation between the laser process parameters and dissimilar laser welding macroscopic measurements (weld bead appearance, weld geometry) was developed to establish a statistical nonlinear model to predict the weld quantitative results and weld quality characterizations.

2- Materials and methods

The materials used in this was nickel base superalloy Inconel 600 and duplex 2205 duplex stainless steel. the martials physical and chemical properties is observed in Table 1. The parts prepared with 25×55 mm in rectangular geometry cut with wire cut cnc machine followed by grinding to remove slags at the weld line contact surface. The Sheath K-type thermocouples with fast thermal response were used to measure the temperature in range of 0~600 ℃. The Advantech USB-4718 thermocouple module with 8-channle was utilized for measuring the temperature during execution of laser welding and the analog response of the thermocouples was converted to temperature data and recorded via LABVIEW software. The special groove on every material with diameter of 1mm and depth of 0.75 mm was engraved through electro discharge machine to locate the thermocouples at specified position. For laser welding a 1000 W fiber laser source connected via QBH connector with laser welding head model Raytools BW240. The argon gas at flow rate between 1.5 and 2.2 lit/min applied to protect the melt pool. Fig.1 depicts the schematic and actual experimental setup of laser welding in accordance to the temperature measurement. For providing the images of the weld bead appearance, the Olympus model SZ-X18 stereoscope was used. The microstructural analysis of the weld bead was performed via Olympus model GX-53 optical microscope and scanning electron microscopy model MIRA SCAN-3 was utilized.

Table 1: Chemical composition of the materials [17,18].

Alloy	Inconel 600	Alloy	Duplex 2205
(%w)			
Cu	0.1	Si	1
Cr	15.5	Mn	2
Mn	0.25	P	0.03
Si	0.2	Al	0.03
Fe	8	Cr	23
C	0.05	Ni	6.5
S	0.002	Mo	3.5
Ni	Balance	S	0.02
		C	0.03

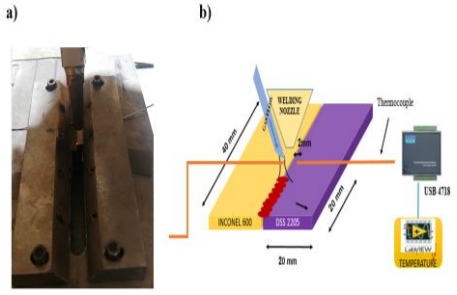

Fig. 1 Dissimilar laser welding experimental setup for a) an actual, b) schematic view

3- Experimental design

Evaluating the laser welding parameters effect on weld geometry and the maximum temperature near the melt pool, the full central composite experimental design composed of four continuous factors is considered to evaluate the weld geometry including depth and width of the fusion zone and the temperature field around the melt pool according to the variation of process parameters. The table.2 illustrates the parameters level selected for laser welding. The processing parameters are including laser power distance of nozzle from the workpiece center, linear welding speed, and deviation of the laser beam. The main matrix of the experiments with random order of executing was shown in table.3. The total number of 28 experiments composed of 4 center points at the same values and 8 axial points on the cube surface were performed to statistically evaluate the process parameters effect on the responses. This research has investigated a set of parameters combinations including focal distance, beam deviation and welding speed on the responses.

Table 2: The parameters levels in variation in dissimilar laser welding process.

No	Focal Distance (mm)	Speed (mm/min)	Power (W)	Deviation (mm)
1	-1.5-+4.5	200-450	200-550	-0.4-+0.4

Table 3: Main matrix of the experiments.

No.	Speed (mm/min)	Power (W)	Focal distance (mm)	Deviation (mm)
1	200	450	0.0	0.2
2	200	450	3.0	0.2
3	400	450	0.0	-0.2
4	400	300	0.0	-0.2
5	300	375	1.5	0.0
6	400	300	3.0	-0.2
7	300	375	1.5	0.0
8	300	375	4.5	0.0
9	400	300	0.0	0.2
10	300	375	1.5	0.0
11	400	450	3.0	-0.2
12	300	525	1.5	0.0
13	300	375	-1.5	0.0
14	450	375	1.5	0.0
15	400	300	3.0	0.2
16	200	300	3.0	-0.2
17	100	375	1.5	0.0
18	300	375	1.5	0.4
19	200	550	0.0	-0.2
20	200	300	3.0	0.2
21	300	225	1.5	0.0
22	200	450	3.0	-0.2
23	200	300	0.0	-0.2
24	300	375	1.5	0.0
25	400	450	3.0	0.2
26	200	300	0.0	0.2
27	300	375	1.5	-0.4
28	400	450	0.0	0.2

4-Results and discussion

This study presents the effect of the different combinations of focal distance, welding speed and beam deviation on the weld bead characterization, weld bead geometry, the maximum temperature at the position of 2mm from the melt pool center and microstructural changes according to the laser heating and cooling cycles from different base metals to the fusion zone of dissimilar joint.

4-1- The parameters effect on the weld melt pool width

According to the Rsq value of 90.8% and lack of fit 0.645, the regression equation of weld width (Eq. (1)) matched well with experimental data. The significant influential linear factors include focal distance and output power of the incident laser beam. The square of beam deviation and focal distance and welding movement speed interaction and deviation of the beam have had the influential effect on the weld width.

(1)

width(mm)=1.0547+ 0.001761 Power(W)- 0.000454 Speed(mm/min)- 0.0408 Focal distance (mm)- 0.361 Deviation (mm)+ 0.03185 Focal distance (mm)×Focal distance (mm)- 1.802 Deviation (mm)×Deviation (mm)- 0.00088 Power(W)×Deviation (mm)+ 0.003719 Speed (mm/min) ×Deviation (mm)- 0.2021 Focal distance (mm) ×Deviation (mm)

In Fig. 2, it can be seen that with the increasing the distance from the focal point position up to 2 mm, the width of the molten pool decreases firstly. The further increase of the focal distance up to 4mm leads to the clear increase of the melt pool width because of the increase in the diameter of the laser incident beam on the workpiece surface. The reduction in density of laser beam energy leads to a significant decrease in the weld penetration depth. Conversely, it is evident that the maximum width of the molten pool created at the junction of two parts where the laser beam is radiated. The reason behind this phenomenon is the efficient melting of

both materials by considering lower laser beam absorbsion of Inconel 600 and duplex 2205 stainless steel higher melting point. In general, the width of the melt pool upper region when transferring the laser beam to the duplex steel was more than that of super alloy 600. The laser beam is absorbed more efficiently by duplex steel, resulting in a greater melting volume and an expansion in the weld bead width. The lowest value of the weld bead width was observed at the focal distance is 2 mm, which means that the effect of reducing the energy density on the width of the molten pool overcomes the increase of the diameter of the laser beam.

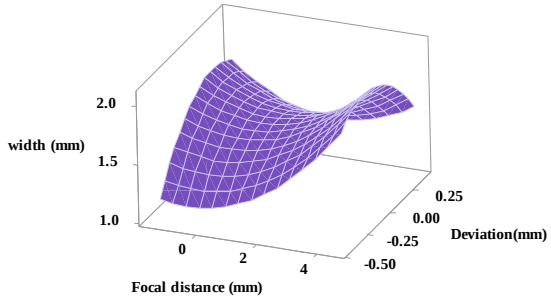

Fig. 2 The focal distance and laser beam deviation effect on the weld width.

Fig. 3 depicts the significant interaction effect of laser beam deviation from the weld centerline and variation in speed of welding on the width of the molten pool. By evident boosting the beam movement speed and beam deflecting in direction of Inconel 600 super alloy, the melt pool width has vividly reduced from 1.6 mm to 1 mm. This is in the case that speed changes do not cause remarkable change in the melt pool width when laser beam is irradiated at the junction of two parts and with the radiation on the duplex steel. Therefore, when the majority of the laser beam irradiated the Inconel 600 with higher speed and lower interaction of laser beam to the materials surface, the melting efficiency of the laser beam reduced about 40%. At high level of welding speed, deviating the beam in direction of Duplex steel increases the width of the molten pool by about 0.6 mm. Lower amount of absorption coefficient for Inconel 600 alloy compared to the duplex steel and also increasing the linear speed of welding have reduced the melting volume index and thus the melt pool width. Meanwhile, with the radiation of the laser beam in the center of the dissimilar joint of two parts or with beam irradiation toward duplex steel, not much changes of the weld width are observed. The biggest changes in the speed of 500 mm/ minute were from Inconel 600 alloy to duplex steel. Hence, it can be concluded that the welding speed has had the most significant influence by the laser beam deviating in direction of Inconel 600 alloy.

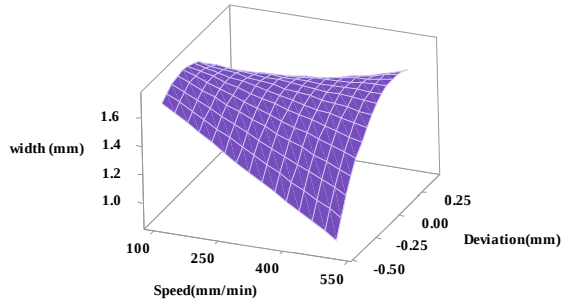

Fig. 3 The laser beam deviation and welding speed effect on the weld width.

It can be seen in Fig. 4 that with the increase in welding speed, the width of the molten pool has slightly decreased. It can be seen that with laser welding, the lowest value of the width of the molten pool is created at the focal point, and with the higher focal distance (augmentation the diameter of the laser beam), the melt pool width becomes larger due to the increase in the diameter of the laser beam. It can be

seen that by more increase in the focal distance up to 4 mm, the width of the molten pool has increased by about 0.5 mm. The maximum rate of increase in speed was at 200 mm/min. The effect of focal length changes on the width of the melt pool is non-linear due to the variation in beam diameter and thereby the beam energy level. The effect of changing the focal distance on the weld width variation is far more than the welding speed about 3 fold.

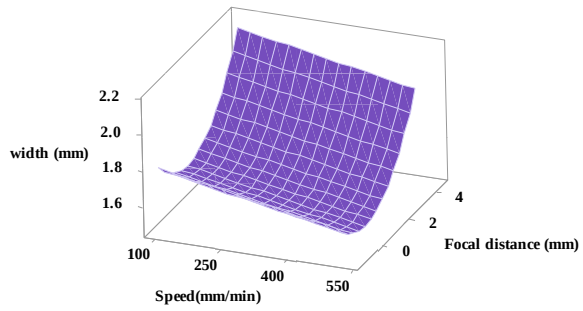

Fig. 4 The welding speed and focal distance effect on the weld width.

Fig. 5 shows a clear comparison of weld width according to the variation of beam deviation, focal distance and speed of welding. The effect of deviating the laser beam on the variation the width of the weld bead is observed in Fig. 5. Through welding at center line of the joint, the produced width reached to the highest value of 1.6mm. By deviating the beam toward duplex side, the weld bead width has reduced to the 1.4mm as shown in Fig. 5b. If the laser beam moved in direction of the Inconel 600, the dimension of the weld bead width noticeably dropped to 1mm, as depicted in Figure 5. Apart from the weld bead width, the appearance of the weld bead and melt volume have slightly changed when the absorbsion of the laser beam changed by deviating toward Inconel 600 alloy.

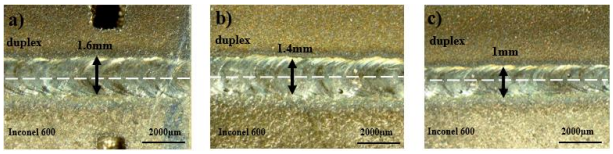

Fig. 5 Effect of deviating the laser beam on the weld bead width and appearance for a) weld center line, b) deviation toward duplex side, c) deviation toward Inconel 600 side.

The effect of focal length variation on the weld bead width is observed in Fig. 6. By welding at focal distance, the resultant width reached to the value of 2mm (See Fig. 6a). The increase in focal length up to the 2mm ends in reduction about 0.4mm as shown in Fig. 6b. more increase of the focal length up to the 6mm has increased the weld bead width more than the focal length position and reached to 2.1mm as it is clearly seen in Fig. 6c. Hence, it can be concluded that increasing the focal length about 2mm not only reduced the laser beam energy density but also reduced the total melting volume during welding process. Furthermore, due to the lower beam diameter size compared to the focal distance of 6mm, the resultant weld bead width is smaller among all.

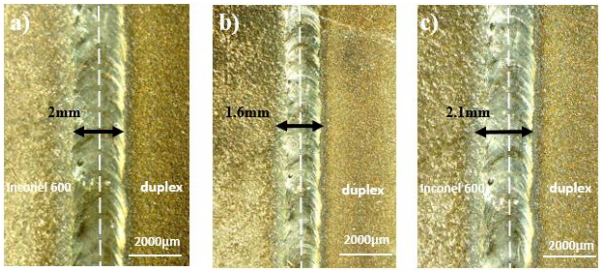

Fig. 6 Effect of focal distance on the weld bead width and appearance at focal length of a)0mm, b) 2mm, c)4mm.

Fig. 7 illustrates the welding speed effect on the width of the weld bead width variation. Compared to the other parameters, variation of welding speed has

had much lower effect on the weld bead width. By increasing the welding speed from 200mm/min to 600mm/min, the width of the weld bead reduced about 0.3mm. Evidently, by increasing welding speed, in addition to decreasing the weld width, the amount of overlapping factor diminished clearly.

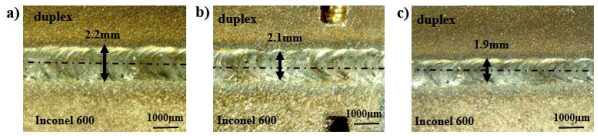

Fig. 7 Effect of welding speed on the weld bead width and appearance for a)200mm/min, b) 400mm/min, c)600mm/min.

4-2- The parameters effect on the melt pool depth

Fig. 8 shows the beam deviation and movement speed effect on melt pool depth. The observation reveals that the most significant reduction in the molten pool depth occurs when deflection of the beam in direction of the duplex steel. The depth of the molten pool decreased by approximately 1mm when the welding speed was raised from 200 mm/min to 450 mm/min, with the redirected towards the duplex steel. In general, with the laser beam deflection in direction of the duplex steel at speed of 200 mm/min, the melt pool depth has been increased by about 0.8 mm. It is evident that at a velocity of 450 mm/min, the molten pool's depth remains relatively constant as the laser beam moves because of lower time of laser beam/metal surface interaction, as well as the inadequate melting. As a result of the laser beam being more absorbed in the duplex steel, it causes the molten pool to have a greater depth as a result of laser beam deflection on stainless steel side.

.

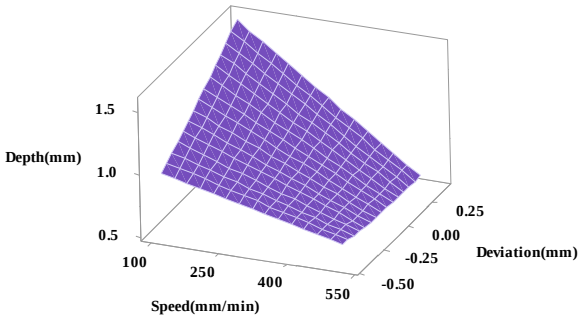

Fig. 8 The welding speed and deviation effect on melt pool depth.

The data presented in Figure 9 highlights that the influence of welding speed on the depth of the molten pool is more significant than that of the focal distance. Specifically, an increase in welding speed from 200 to 450 mm/min led to a decrease of around 0.6 mm in the depth of the molten pool. By increasing the focal distance to 4 mm, the changes in the melt pool depth are very minor. By increasing the speed at the focal distance of 4 mm, the melt pool depth decrease rate is higher up to 0.9 mm. As a result of decreasing the energy density of the laser beam and the reduced efficiency of melting at high speeds, the depth of the molten pool is considerably diminished when the focal distance is set at 4 mm. Changes in the focal distance in each of the examined levels do not have much effect on the melt pool depth changes.

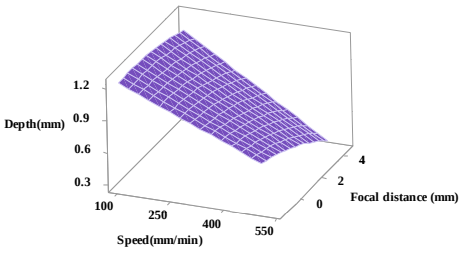

Fig. 9 The welding speed and focal distance effect on the melt pool depth.

The effect of focal length and deflection of the laser beam on melt pool penetration depth of the is clearly observed in Fig. 10. When the laser beam is directed towards the Inconel 600 alloy with an increased focal distance, the melt pool penetration depth has been reduced by approximately 0.6 mm. Also, the rate of reduction of the depth of the molten pool has the maximum value at focal length of 4 mm.

When welding was carried out at focal point position of the beam, the melt pool depth remained relatively constant because of high laser beam energy density. As a result, the laser beam was able to penetrate nearly the entire thickness of the workpiece. By adjustment of the focal length and especially the beam deviation in direction of Inconel 600 super alloy, the depth of the molten pool has decreased by about 50 percent. With the deflection of the laser directed to the Inconel 600 due to a lower efficiency of laser beam absorption for Inconel 600 and a significant reduction in energy density with increasing focal length, the beam penetration has been remarkably reduced. The maximum melt pool depth value is created at a focal length in case the laser beam is majorly irradiated on the duplex steel.

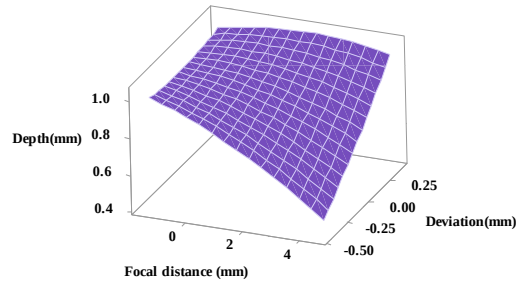

Fig. 10 The effect of beam deviation and focal distance on melt pool depth.

4-3-Comparison the parameters effect on the temperature at the region near the fusion zone on each material

In Fig. 11, the variation of the peak temperature around the region near the melt pool according to the variation of focal length and laser beam deflection is observed. Fig. 11 illustrates that by increasing the focal length and reducing the energy density of the laser beam, the temperature of Inconel 600 alloy has decreased from 180°C to 80°C. The highest temperature value for Inconel 600 is in the center of the connection, while the highest temperature for duplex steel is created by transferring the laser beam by 0.2 mm towards it (see Figs. 11a and b). Changing the focal length significantly impacts the temperature variations of Inconel600 alloy when the laser beam is redirected towards it. When the laser beam deviates towards the duplex steel, the temperature recorded by the thermocouples rises. Shifting the laser beam by 0.2 mm towards the duplex steel results in an augmentation in the melting volume and temperature, as well as a closer proximity to the point where the laser beam intersects near the tip of the thermocouple. The highest temperature value achieved at the focal length of 2 mm, and as the focal length increases, the temperature surrounding the molten pool decreases.

Fig. 12 illustrates the welding speed and focal length impact on the temperature of Inconel 600 alloy. It can be seen that welding speed variation do not have much effect on the rate of temperature reduction around the molten pool in Inconel 600 alloy while the duplex temperature remarkably changed. It is clearly seen that the maximum temperature created in the focal length is 2 mm, which has sufficient melting volume and the lower distance of the laser beam from the temperature measurement point. With the increase in focal length, the rate of temperature

decrease rises, while the energy density of the laser beam decreases significantly due to the larger diameter of the beam. For duplex steel, it can be seen that at a focal distance of 2 mm, the highest temperature around the molten pool has been created as shown in Fig.12. It can be seen that the effect of the process of welding speed changes on the temperature changes of duplex steel is linear if the focal length changes have a non-linear trend. However, it is evident that as the welding speed increases and consequently the volume of the molten pool decreases, the most significant temperature variation occurs at a welding speed of 200 mm/min.

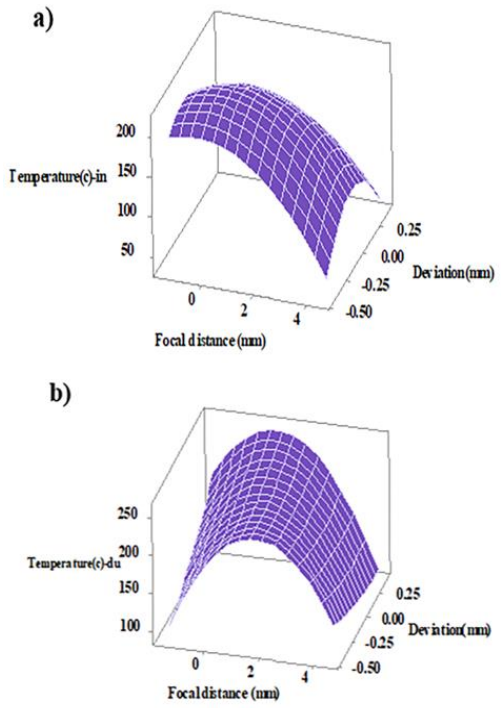

Fig. 11 The effect of beam deviation and focal distance on the temperature of a) Inconel 600, b) duplex stainless steel.

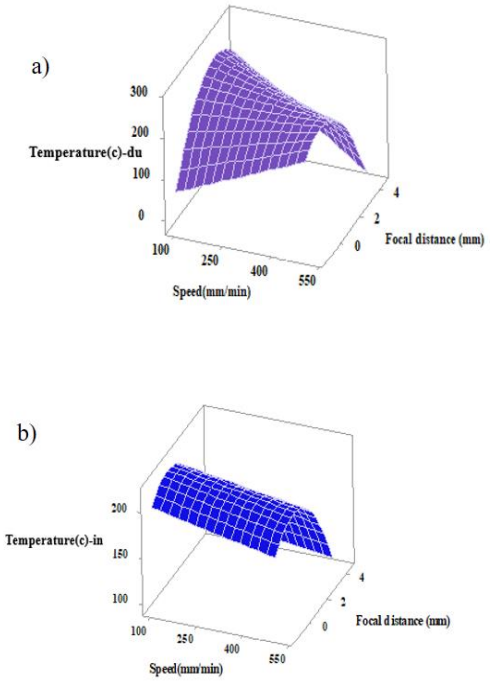

Fig. 12 The effect of focal distance and welding speed on the temperature of a) Inconel 600, b) duplex stainless steel.

Fig.13 shows some samples for measuring the melt pool depth according to the metallography analysis. The maximum penetration depth of the fusion was measured and considered as means of the melt pool depth.

Fig. 14 illustrates a comparison of the measured temperature for Inconel 600 and duplex 2205 steel. it is clearly observed that the maximum temperature for duplex steel is vividly higher than Inconel 600 about 20°C at a distance of 2mm from the melt pool center. The cooling rate of duplex is slightly higher than Inconel 600 because of reduction from the high temperature point to the room temperature at lower time. Due to the higher melting volume of Inconel 600 and lower melting point temperature, the time of cooling for Inconel 600 side is clearly higher in comparison to duplex steel.

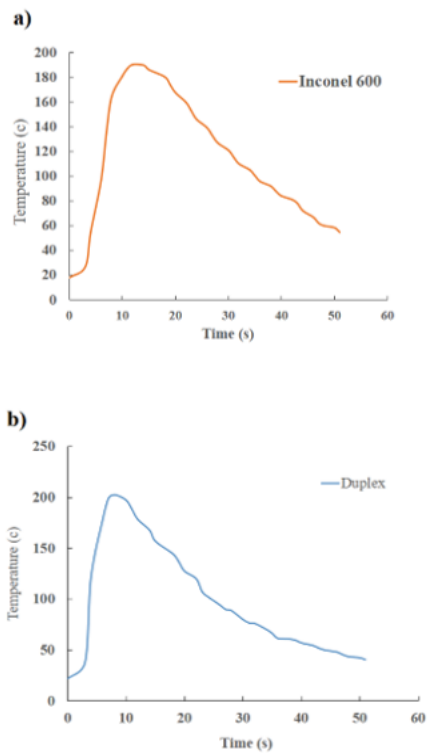

Fig. 13 The measured temperature during welding process for a) Inconel 600, b) duplex 2205

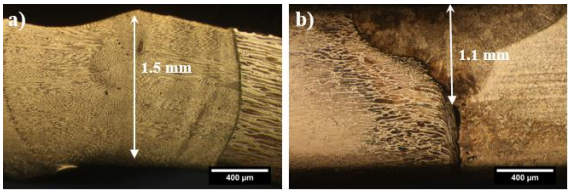

Fig. 14 The melt pool depth at laser power of 450 W and focal distance of 0mm and welding speed of a)200mm/min, b)400mm/min.

4.4-Microstructure analysis of the fusion zone and boundary regions of the base metals

The microstructural analysis of different areas from the base metals to the dissimilar fusion zone region shown in Fig. 15 was analyzed according to the temperature gradient form the heat input of the laser beam toward the cooling rate induced by dissimilar materials. At the region near the heat affected zone of Inconel 600 alloy shown in Fig.15b, an evident grain growth is observed at this region where lower heating intensity and higher cooling rate existed. On the contrary, only a slight changes of the portion of ferrite to austenite are observed at the region near the heat affected zone of duplex steel. As it is observed in Figs.15 e and 15d, the fusion zone microstructure composed of cellular and columnar microstructure depends on the temperature gradient at different regions of the fusion zone. furthermore, the interdendritic microstructure is observed at some regions of the fusion zone as illustrated in Fig.15f.

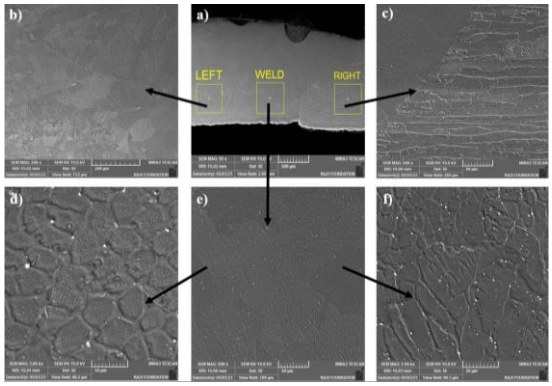

Fig. 15 Microstructure of the weld fusion zone and adjacent areas near the melt pool.

The laser welding parameters effect on the weld characterizations such as weld geometry and fusion zone microstructure was investigated. It can be concluded that the higher laser power produced more penetration rate and higher volume of melted material although due to the having different chemical and physical properties, the martials participation on formation of dissimilar weld joint has been different because of having different thermophysical properties. On the other hand, the fusion zone microstructure composed of mainly from Inconel 600 alloy has had different microstructural and mechanical properties compared with only Inconel 600 alloy welding. The major issue with the mechanical properties of the weld joint is

formation of unmixed layer toward duplex side which in turn reduced the joint tensile strength because of insignificant melting of duplex alloy at the fusion line with the melt pool.

5- Conclusion

This study presents the experimental results of dissimilar laser welding process by variation the welding speed, beam deviation and focal distance on the responses of weld bead width and depth, temperature near the melt pool of each material and microstructural changes.

The width of the melt pool in duplex steel was found to be greater than that in super alloy 600 when the laser beam was transferred. This is attributed to the higher absorption coefficient of the laser beam in duplex steel, which leads to a higher melting volume and ultimately an increase in the width of the molten pool.

When the welding process was carried out at the focal point, the melt pool depth remained relatively constant because of high laser beam energy density. As a result, the laser beam was able to penetrate nearly the entire thickness of the workpiece.

The melt pool penetration depth has been reduced by approximately 50 percent by increasing the focal length and specifically altering the laser beam's deviation in direction of the Inconel 600 super alloy. The highest melt pool penetration depth occurs when the laser beam is directed onto the duplex steel at a specific focal length.

Due to the lower absorption coefficient and an increase in focal length in case the laser beam directed towards the Inconel 600, a significant decrease in energy density is observed. Consequently, the melt pool depth has been notably diminished.

The maximum width of the molten pool occurs at the place of laser beam radiation at the junction of two parts. The reason behind this phenomenon is the efficient melting of both materials by considering lower laser beam absorbsion of Inconel 600 and higher melting point of duplex 2205 stainless steel.

At the heat affected region of Inconel 600 alloy, an evident grain growth is observed at this region where lower heating intensity and higher cooling rate existed. On the contrary, only a slight changes of the portion of ferrite to austenite are observed at the region near the heat affected zone adjacent to duplex steel fusion line.

The maximum temperature for duplex steel is vividly higher than Inconel 600 about 20°C at a distance of 2mm from the melt pool center at the place the thermocouples measured the temperature. Therefore, due to the higher melting point of duplex stainless steel and higher thermal conductivity, the higher temperature near the melt pool is gained.

References

[1] Ma, G., Wu, D., & Guo, D. (2011). Segregation characteristics of pulsed laser butt welding of Hastelloy C-276. *Metallurgical and Materials Transactions A*, *42*, 3853-3857.

[2] Lienert, T. J., Burgardt, P., Harada, K. L., Forsyth, R. T., & DebRoy, T. (2014). Weld bead center line shift during laser welding of austenitic stainless steels with different sulfur content. *Scripta Materialia*, *71*, 37-40.

[3] Hejripour, F., & Aidun, D. K. (2017). Consumable selection for arc welding between Stainless Steel 410 and Inconel 718. *Journal of Materials Processing Technology*, *245*, 287-299.

[4] Guo, Y., Wu, D., Ma, G., & Guo, D. (2014). Trailing heat sink effects on residual stress and distortion of pulsed laser welded Hastelloy C-276 thin sheets. *Journal of Materials Processing Technology*, *214*(12), 2891-2899.

[5] Li, Y., Xu, H., Zhu, F., & Wang, L. (2014). Low temperature anodic nitriding of AISI 304 austenitic stainless steel. *Materials Letters*, *128*, 231-234.

[6] Wu, D., Cheng, B., Liu, J., Liu, D., Ma, G., & Yao, Z. (2019). Water cooling assisted laser dissimilar welding with filler wire of nickel-based alloy/austenitic stainless steel. *Journal of Manufacturing Processes*, *45*, 652-660.

[7] Naffakh, H., Shamanian, M., & Ashrafizadeh, F. (2009). Dissimilar welding of AISI 310 austenitic stainless steel to nickel-based alloy Inconel 657. *Journal of materials processing technology*, *209*(7), 3628-3639.

[8] Zhou, S., Ma, G., Chai, D., Niu, F., Dong, J., Wu, D., & Zou, H. (2016). Nickel-based alloy/austenitic stainless steel dissimilar weld properties prediction on asymmetric distribution of laser energy. *Optics & Laser Technology*, *81*, 33-39.

[9] Dev, S., Ramkumar, K. D., Arivazhagan, N., & Rajendran, R. (2018). Investigations on the microstructure and mechanical properties of dissimilar welds of inconel 718 and sulphur rich martensitic stainless steel, AISI 416. Journal of Manufacturing Processes, 32, 685-698.

[10] Cheng, B., Wu, D., Yue, K., Ma, G., & Niu, F. (2022). Effect of low-temperature cooling on corrosion properties of laser welding Hastelloy C-276/304 stainless steel with filler wire. *Optics & Laser Technology*, *148*, 107755.

[11] Kumar, G. S., Saravanan, S., & Raghukandan, K. (2021). Effect of heat input on microstructure and mechanical properties of laser welded dissimilar grade nickel alloys. *Optik*, *248*, 168106.

[12] Kumar, G. K., Velmurugan, C., Jayaram, R. S., & Manikandan, M. (2020). Effect of laser welding process parameters on dissimilar joints of AISI 316 and nickel 201. *Materials Today: Proceedings*, *22*, 2964-2973.

[13] Sunder, S. S. S., & Dewangan, S. (2024). Critical analysis into mechanical properties and microstructure of dissimilar welded joint between stainless steel-304 and Inconel-718. *Journal of The Institution of Engineers (India): Series D*, *105*(2), 853-861.

[14] Bhanu, V., Fydrych, D., Gupta, A., & Pandey, C. (2021). Study on microstructure and mechanical properties of laser welded dissimilar joint of P91 steel and INCOLOY 800HT nickel alloy. *Materials*, *14*(19), 5876.

[15] Dak, G., & Pandey, C. (2021). Experimental investigation on microstructure, mechanical properties, and residual stresses of dissimilar welded joint of martensitic P92 and AISI 304L austenitic stainless steel. *International Journal of Pressure Vessels and Piping*, *194*, 104536.

[16] Thejasree, P., Manikandan, N., Raju, R., Narasimhamu, K. L., Surendranatha, G. M., & Damodaram, A. K. (2022). Investigations on laser beam welded Inconel 718 weldments. Materials Today: Proceedings, 68, 1757-1761.

[17] ASM Handbook (2008), volume 24A, Chapter 7: Duplex Stainless Steels.

[18] ASM Handbook (1990). Volume 2: Properties and Selection: Nonferrous Alloys and Special-Purpose Materials, ASM International.